nanomaterials

MDPI

Article

Adding Nano-TiO_2 to Water and Paraffin to Enhance Total Efficiency of a Photovoltaic Thermal PV/T System Subjected to Harsh Weathers

Miqdam T. Chaichan [1], Hussein A. Kazem [2], Ahmed A. Alamiery [3,*], Wan Nor Roslam Wan Isahak [3], Abdul Amir H. Kadhum [4] and Mohd S. Takriff [3,5]

1 Energy and Renewable Energies Technology Center, University of Technology-Iraq, Baghdad 10001, Iraq; miqdam.t.chaichan@uotechnology.edu.iq
2 Faculty of Engineering, Sohar University, P.O. Box 44, Sohar 311, Oman; h.kazem@su.edu.om
3 Department of Chemical and Process Engineering, Faculty of Engineering and Built Environment, Universiti Kebangsaan Malaysia (UKM), Bangi 43600, Malaysia; wannorroslam@ukm.edu.my (W.N.R.W.I.); sobritakriff@ukm.edu.my (M.S.T.)
4 Faculty of Medicine, University of Al-Ameed, Karbala 56001, Iraq; amir1719@gmail.com
5 Chemical and Water Desalination Engineering Program, Department of Mechanical & Nuclear Engineering, Collage of Engineering, University of Sharjah, Sharjah P.O. Box 27272, United Arab Emirates
* Correspondence: dr.ahmed1975@ukm.edu.my or dr.ahmed1975@gmail.com

Abstract: Iraq is characterized by hot and sunny weather with high radiation intensity. These conditions are suitable to produce photovoltaic electricity, on the one hand, but on the other hand are not suitable for photovoltaic modules whose efficiency decreases with increasing temperature. In this study, a photovoltaic module was practically cooled by two PV/T systems, one cooled by water and the other by nanofluid and nano-paraffin. Iraqi-produced paraffin was used in this study for its cheap price, and because its melting and freezing temperature (46 °C) is close to the operating range of photovoltaic modules. Nano-TiO_2 was adopted as an additive to water and paraffin. The study results showed an obvious enhancement of the thermal conductivity of both water and paraffin, by up to 126.6% and 170%, respectively, after adding a 2% mass fraction of nano-TiO_2. The practical experiments were carried out outdoors in the city of Baghdad, Iraq. A fluid mass flow rate of 0.15 kg/s was selected for practical reasons, since at this rate the system operates without vibration. The PV panel's temperature, in the PV/T system (nano-fluid and nano-paraffin), decreased by an average of 19 °C when the tested systems operated during the peak period (12 PM to 3 PM). The decrease in temperatures of the PV module caused a clear improvement in its electrical efficiency, as it was 106.5% and 57.7% higher than the PV module (standalone) and water-cooled PV system, respectively. The thermal efficiency of this system was 43.7% higher than the case of the water-cooled PV/T system. The proposed system (nano-fluid and nano-paraffin) provides a greater possibility of controlling the heat capacity and increasing both efficiencies (electrical and thermal), when compared to a standalone PV module, in harsh Iraqi weather.

Keywords: additives; paraffin; PV/T system; nano-fluid; nano-paraffin

Citation: Chaichan, M.T.; Kazem, H.A.; Alamiery, A.A.; Isahak, W.N.R.W.; Kadhum, A.A.H.; Takriff, M.S. Adding Nano-TiO_2 to Water and Paraffin to Enhance Total Efficiency of a Photovoltaic Thermal PV/T System Subjected to Harsh Weathers. *Nanomaterials* **2022**, *12*, 2266. https://doi.org/10.3390/nano12132266

Academic Editor: Andreu Cabot

Received: 10 January 2022
Accepted: 10 February 2022
Published: 30 June 2022

1. Introduction

The typical Iraqi citizen suffers from poor services in general and a severe shortage of electricity supply. Starting from 2003 till today, Iraqi citizens often use diesel generators extensively to fill the severe shortage of supplied electricity, especially after 2003. This focus on using such generators, without limits on the pollutants emitted by them, caused high levels of air pollution and noise rates [1]. Meanwhile, the sharp rise in the use of vehicles and trucks, due to the failure of the public transportation system, led to a doubling of the concentrations of many pollutants emitted from car exhaust [2]. The Iraqi government tends to, as a primary solution to the problem of air pollution, rely on building renewable

electricity generation plants using photovoltaic cells. The Iraqi government is considering deploying 17 solar-powered power plants in different parts of the country, as shown in Table 1 [3]. However, the climatic conditions of this country, namely a significant rise in suspended dust in the air, as well as the continuous recurrence of dust storms, limit this trend towards the use of PV modules technology. Many research studies have put forward several suggestions to solve these problems. Many studies have emphasized the periodic cleaning of PV modules with various types of cleaning materials, according to the region and the human activities within it [4–6].

Table 1. Suggested solar energy stations with its details.

Governorate	Station Location	Designed Power (MW)	Voltage Level (KV)
Al-Muthana	Sawa-1	30	33
Al-Muthana	Sawa-2	50	132
Al-Muthana	Khidhir	50	132
Karbala	Karbala	300	132
Babilon	Al-Iskandaria	225	132
Diwania	Ramla	50	132
Wassit	Jassan	50	132

One of the reasons for the delay in installing these systems is that the performance of the photovoltaic modules deteriorates when the PV module temperature increases. The rise in PV panel temperature is largely from the solar radiation falling on it that is converted into heat, increasing the panel temperature, while a small part of this radiation is used to generate electricity [7]. Therefore, lowering the temperature of the PV modules enables them to operate close to their optimum performance. The researchers studied several methods of cooling PV modules such as air [8], water [9], nanofluids [10], PCMs [11], and nano-PCM cooling [12]. In the past decade, most researchers have emphasized the use of PV/T systems, which combine a photovoltaic module and a thermal collector. In this system, a heat exchanger (thermal collector) absorbs the excess heat in the photovoltaic body and delivers it to another application using a cooling fluid [13].

The literature is littered with several designs that have been suggested for cooling PV modules to improve their performance. Reference [14] used water to cool the PV/T system and improve its electrical efficiency. The authors confirmed a clear improvement in efficiency compared to the independent photovoltaic module. Reference [15] proposed the use of nanofluid, which is a base fluid, in water, with nanoparticles added to it, to enhance heat transfer rate from the PV module body to a thermal collector. This method has been studied in detail by many researchers, using many types of nanoparticles, with metallic and non-metallic sources, to discover the best fluids to use in PV/T systems for optimal performance [16–18]. Many studies have also focused on evaluating several types of base fluid, and examining their effects on the rate of heat transfer [19–21]. Most of the studies showed that water can be considered as one of the best of these basic fluids, because most of its thermal properties are suitable for PV/T applications [21].

Phase change materials store thermal energy when they undergo a change of state (phase) from solid to liquid, or vice versa. The heat stored, in this case (phase change), is latent heat, and this process is called the charging process, during which this material melts when its temperature reaches the melting point (the temperature of its phase change) [22]. The temperature of the substance remains constant until the end of the melting process. When the molten material is cooled, it begins to release the heat stored in it during the vacuum process [23]. Researchers have taken advantage of this property in many solar energy applications. In such applications, the temperature fluctuates due to the oscillation of the incident radiation from sunrise to sunset, and the interruption of heat when the sun is absent. Therefore, researchers have used PCMs in solar thermal applications to store heat in solar stills [12,24], air heaters [25,26], and PV/T systems [27,28]. Many phase change materials are available, each with different melting and hardening points, ranging from

5 °C to 190 °C. These materials store latent heat about 5 to 14 times as much as sensible heat storage materials, such as water, pebbles, or rocks [29].

Paraffin is one of the PCM families, and at room temperature takes the form of wax, which is formed of hydrocarbons produced in the distillation of crude oil. Paraffin wax is one of the most important types of PCM used in research for heat storage applications [30], because it is cheap and can store moderate heat energy, but it is criticized for its low thermal conductivity (TC) [30]. In general, paraffins are safe, affordable, non-irritating, and have a wide range of melting and solidification temperatures making their use possible in many latent heat storage applications. These materials are chemically inactive and stable. In addition, applications using paraffin for heat storage maintain high stability of melt-hardening cycles over very long periods [31]. As for some properties that may be considered undesirable, such as low TC, melting temperatures, and moderate flammability, they can be partially treated by adding additives such as nanoparticles or paraffinic materials.

Reference [32] used TRNSYS, with empirical confirmation of the extent of the decrease in the surface temperature of the PV panel, because of adding PCM to the PV/T system. The low TC of paraffin has been identified as one of the drawbacks that could limit their use in PV/T systems [33]. Therefore, several studies have suggested adding high TC nanoparticles to paraffin to improve the low TC of these materials [34,35].

Most nanoparticles, especially metallic ones, are characterized by their high TC [36–38]. Therefore, adding nanoparticles to the base fluid or paraffin will significantly improve their TC. However, these particles must be added in limited weight or volume ratios, as increasing their percentage in the basic fluid or paraffin will greatly reduce the stability of the nano-fluid or nano-paraffin [39]. Stability means the persistence of the thermophysical properties of a nanofluid or nano-paraffin for a long time. This is achieved by ensuring that nanoparticles do not collect and clump, and then precipitate for a period of time, instead remaining suspended in the base fluid or paraffin. The agglomeration of nanoparticles causes an increase in their mass, which causes their sedimentation, and, as a result, there is a clear decrease in the TC of the nanofluid or nano-paraffin [40]. The mixing process can be considered costly in terms of material, as well as in terms of the time it takes [41]. Ghademi et al. [42] considered that van der force is responsible for the agglomeration and deposition of these nanoparticles. Reference [33] confirmed that the deposition of nanoparticles causes the deterioration of the quality of the nanofluid. Therefore, ensuring the stability of nano-mixtures (whether nanofluids or nano-paraffin), and their uniform distribution within these mixtures, is a key factor in the quality of the nano-product.

The best way to mix nanoparticles with a base fluid or paraffin, which most researchers recommend, is to use ultrasonic vibration with the addition of a surfactant to the base fluid or molten paraffin, to achieve a product with good stability, i.e., stable for a long period of time [43]. Numerous experimental studies that used this method found it very effective, and the researchers were able to obtain nano-products with acceptable stability. Some researchers emphasized the sonication time and considered it a key factor in achieving a stable nano-product. It can be said that all studies did not agree on a specific time for sonication, and this is normal, as there are many differences, such as the base materials or the quality of the added nanoparticles, which could cause such differences. Afzal et al. [43] confirmed this matter, as they considered that the time of the sonication process is determined by the type of nanofluid, especially the added nanoparticles, i.e., the percentage, shape, and size of the particles. Chen et al. [44] mixed nanoparticles with water with several periods of sonication (2 h and 45 min, 3 h and 15 min, and 3 h and 45 min). The authors found that the optimal sonication time for the prepared liquids was 3 h and 15 min.

Thermophysical properties determine the rate of heat transfer by the nanofluid or nano-paraffin. These properties can be specified as TC, viscosity, density, and specific heat [45]. These properties change with the temperature of the nanofluid or nano-paraffin, which determines the efficiency of their performance in the heat transfer process [46–48]. In addition to the temperature of the nano-product, other factors determine the quality of its

thermophysical properties (including, but not limited to, the type of base liquid, the type of nanoparticles used, the temperature range of application, the sonication period used to prepare the nanofluid, and the percentage of nanoparticles added to the base fluid) [49–51]. Researchers have not yet agreed on a clear definition of the effect of any of these factors on the thermophysical properties of nanofluid and nano-paraffin. Therefore, researchers continue to evaluate and study these factors to this day, aiming to determine the optimal nano-fluid and nano-paraffin for use in solar heat transfer applications.

In this empirical study, the use of PV/T systems in the harsh environmental conditions of Iraq for cooling PV modules was investigated. The PV/T system was designed in the form of a tank, filled with paraffin, attached to the PV panel at the back to absorb excess heat from it and reduce temperature fluctuation on its surface. Inside the wax, a heat exchanger was dipped, through which a nanofluid with high TC circulated, which in turn absorbed the heat collected in the paraffin and expelled it out of the system. The objective of this study was to improve the electrical efficiency of the PV/T system and make it suitable for working in harsh and hot weather conditions, such as those in Iraq.

2. Materials and Methods

Figure 1 details the practical steps involved in the study, starting from the selection of materials and preparation of nanofluids and nano-paraffin, to the tests that were carried out on them, as well as the measurements taken from the systems, which will be explained in detail in the following paragraphs.

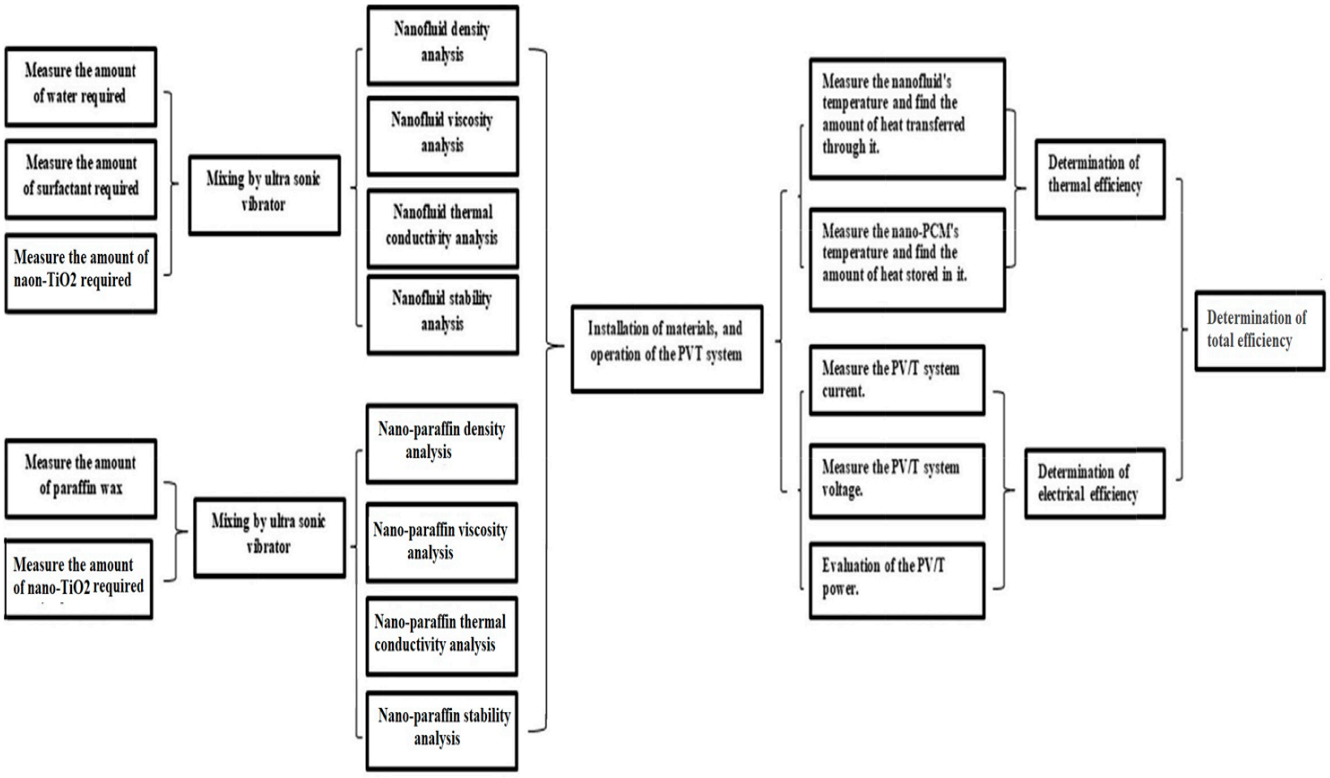

Figure 1. Block diagram for practical steps conducted in the study.

2.1. PV/T System

In this study, a nano-paraffin tank was designed, fabricated, and attached to the PV panel's (Table 2) backside. Inside this tank, a heat exchanger (Figure 2A) was placed to circulate the coolant, which absorbs the heat stored in the paraffin, perpetuating the heat transfer process from the PV to the paraffin (Figure 2B). This tank was connected to the photovoltaic module by welding. The space between the tank surface and the back of the module was filled with silicone oil, to facilitate the heat transfer process and ensure

that no air gaps occurred that could prevent or reduce this transfer. The studied system consists of three photovoltaic modules; one of them is standalone, the second is a PV/T water-cooled system, and the third is heated with nano-paraffin and nano-fluids. The photovoltaic panels were all set facing south at an angle of 33°, to suit the Baghdad city location. The studied system also contains two water pumps to circulate the water and nanofluid, a container for the nanofluid, a data acquisition system, and a laptop computer. The paraffin container was insulated on all sides exposed to the air using insulation (glass wool, 2.5 cm thick) to conserve all heat energy absorbed from the PV panel. For consistency of results, accounting for the fact that the experiments were carried out outdoors, data collection, from measurements of all three systems, was carried out at the same time.

Table 2. Specifications of the PV modules used in the study.

Electrical Properties (Standard Test Conditions)	Symbol	Specification
Model	-	STF–120P6
Max. power	Pmax	120 ± 3%
Voltage (Open-circuit)	Voc	22 V
Current (Short-circuit)	Isc	7.63 A
Voltage at maximum power	VMP	17.40 V
Current at maximum power	IMP	6.89 A
Max. electrical efficiency	$\eta_{ele.}$	14%

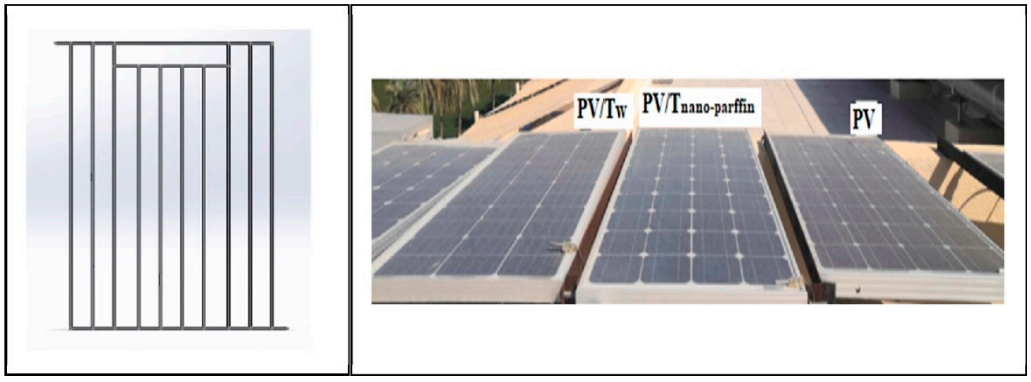

(**A**) (**B**)

Figure 2. (**A**) nanofluid heat exchanger, and (**B**) the studied systems.

The performance of the treadmill systems was calculated using the following equations.

1. Collected thermal energy:

$$Q_u = \dot{m} C_p (T_o - T_i)$$

where Q_u is the useful thermal energy gained from the water or nanofluid, C_p is the water or nanofluid specific heat (J/kg K), and T_o and T_i are the outlet and inlet temperatures, respectively.

2. The PV/T system thermal efficiency:

$$\eta_{th} = \frac{Q_u}{I_s \times A_{co}}$$

where η_{th} is the thermal efficiency, I_s is the solar radiation intensity, and A_{co} is the collector surface area.

3. Electrical power (W):

$$P = I \times V$$

where P is the electrical power, I is the electrical current, and V is the voltage.

4. Electrical efficiency:

$$\eta_{el} = \frac{P}{I_s \times A_p}$$

where η_{el} is the electrical efficiency, P is the power, I_s is the solar radiation intensity, and A_p is the PV panel area.

5. The total efficiency:

$$\eta_t = \eta_{el} + \eta_{th}$$

where η_t is the total efficiency.

2.2. Materials

The choice was made to use nano-TiO_2, which has an acceptable TC; it was added to Iraqi paraffin, which is available in local markets, to form nano-paraffin, and to water, to form a nanofluid. The paraffin used is affordable (US$2/kg). Nano-$TiO_2$ has important properties, such as chemical stability, high surface area, suitable electronic band structure, and high quantum efficiency. This type of nanoparticle has been used in applications such as dyes for photovoltaic cells, biomedical implants, and other applications [52,53]. Nano-TiO_2 is available in local markets at a price of less than US$2/g [54,55]. Table 3 lists the properties of the nano-TiO_2 used in this study. Table 4 illustrates the characteristics of the paraffin used in the practical tests.

Table 3. Nano-TiO_2 specifications.

Item	Nano-TiO_2
Manufacturer	Hongwu Nanometer
Appearance	White colored powder
Purity	99.7%
pH	7.4
Grain size (nm)	20–50 nm
Density (g/cm^3)	3.92
Loss when dried %≤	0.23
Zeta potential (mV)	38.5
Molar mass (g/mole)	79.87
Melting point (°C)	1843
TC (W/m K)	280–750

Table 4. Iraqi paraffin properties [56,57].

Property	Range	Units
Chemical composition	C20H42-C27H56	-
The temperature of melting point	43.5	°C
Liquid state density	836	kg/m^3
Solid state density	929	kg/m^3
Latent heat	197	kJ/kg
Solid state TC	0.21	W/m·K
Liquid state TC	0.19	W/m·K
Liquid state specific heat	2.15	kJ/kg K
Solid state specific heat	2.23	kJ/kg K

The nanoparticles were prepared by placing them in an oven at a temperature of 220 °C for 15 min, to remove any moisture that might be present. This drying process is important in confirming that there is no interconnection between nanoparticles due to moisture before adding them to paraffin or water, in any proportion, even a very small amount. The same mass fraction of nanoparticles was added to water and paraffin (0.5%, 1.0%, 1.5%, and 2.0%). A sensitive balance (type EJ6I0-E) with a measurement accuracy of 0.0001 g was used.

2.3. Preparation of Nano-Paraffin

The paraffin was heated to 60 °C and placed in a container inside a bath that vibrated at ultrasonic speed, while keeping the paraffin hot throughout the mixing period, to eliminate the impact of its viscosity on nanoparticle diffusion. Nano-TiO_2 particles were gradually added to the vibrating liquid paraffin while the sonication process continued, for two consecutive hours without stopping. In this study, an ultrasonic vibrator (type TELSONIC ULTRASONICS CT-I2) with a 12-L bath and an electrical heater with a capacity of 800 W was used. This vibrator could vibrate the fluid in the bath with a maximum frequency of 80 kHz. The sonication time was extended in the preparation of nano-paraffin to ensure a wider spread and optimal distribution of nanoparticles through the paraffin, which hinders future agglomeration. This process succeeded in several studies, and was praised and considered the best method for mixing nanoparticles with PCM [56].

It could be confirmed that the mixing process was successful by seeing the paraffin's color completely changed and without impurities, indicating that the nanoparticles spread through it and were not deposited. Completely changing the color of paraffin without impurities is an indicator of good diffusion of nanoparticles in paraffin.

2.4. Preparation of Nanofluid

Several measures must be taken to ensure that a sufficiently stable nanofluid is prepared. The steps of mixing nano-TiO_2 with water used by reference [51] were adopted. Nano-TiO_2 was added to the water in the same ultrasonic shaker that was previously used to prepare nano-paraffin. The mixing process here lasted longer than the previous case, as the ultrasonic shaking continued for three and quarter and hour, to ensure the best diffusion of nanoparticles in the suspension [44]. The study also relied on adding 0.1 mL of surfactant (Cetyl Trichromyl Ammonium Bromide (CTAB)) to the water to ensure higher stability of the suspension. In this study, the results of reference [57] were used to inform the mixing method, the amount of surfactant added, and its type.

2.5. Uncertainty Analysis

In practical studies, uncertainty analysis is very important to ensure the validity of the measured data. Uncertainty is analyzed through practical calibration of all measuring devices, such as thermocouples, and measurement of thermophysical properties (viscosity, density, heat capacity, and TC). Instruments were calibrated and their results compared with a standard instrument; the deviation from the standard readings was considered an uncertainty [58]. Table 5 shows the details of the measurement tools used and the uncertainty for each. The study uncertainty was assessed by employing the Kline and McClintock equation [58]. The TC and heat capacity were measured using a KD2 Pro-Analyzer, while, for density measurements, a Density tester (type DII-300 L) was employed. A Brookfield programmable viscometer (model: LVDV-III) was used to measure both prepared materials viscosities, while a Zeta-Sizer Nano Analyzer (ZSN) was used to measure the prepared nanofluids' Zeta potentials.

Table 5. The details and uncertainties of the measuring devices used in the tests.

Measured Specification	Device	Uncertainty
Density	Density tester type (DII-300 L)	±0.16
Viscosity	Brookfield programmable viscometer (model: LVDV-III)	±0.12
TC	KD2 Pro-Analyzer	±0.8
Heat Capacity	KD2 Pro-Analyzer	±0.94
Temperatures	Thermocouples type K	±0.93
Weight	Delicate balance type (EJ6I0-E)	±0.34
Coolants flow rate	HC (US Hunter)	±0.55
Stability	Zeta-Sizer Nano Analyzer (ZSN)	±0.88

The results show that the uncertainty of the measurements of the current study was less than 5%, which means that the accuracy of the measurements made is geometrically acceptable. In addition, each experiment was repeated three times to ensure repeatability, and the arithmetic mean of the results was taken.

$$W_R = \left[\left(\frac{\partial R}{\partial x_1} w_1\right)^2 + \left(\frac{\partial R}{\partial x_2} w_2\right)^2 + \ldots + \left(\frac{\partial R}{\partial x_n} w_n\right)^2\right]^{0.5}$$

Hence, the experiments in the study are provided as below:

$$W_{R_1} = \left[(1.16)^2 + (0.72)^2 + (0.8)^2 + (1.04)^2 + (1.3)^2 + (0.94)^2 + (0.55)^2 + (0.88)^2\right]^{0.5} = 3.42$$

3. Results and Discussion

Figure 3 shows photographs of samples of the used paraffin and nano-paraffins. The far left shows a sample image of the Iraqi paraffin used in the study, which has an average melting point of 46 °C. This paraffin is light brown, due to the low number of hydrocarbons in its chemical composition (it did not exceed 20 carbon atoms) and its low oil content. When adding nano-TiO_2 in the smallest amount (0.5%), its color changes to white, and it becomes whiter with increasing mass fractions of added nanoparticles. If all paraffin turns white, this means complete and successful mixing; the presence of points or areas of light brown color means the mixing was a failure, and there is a need to repeat the sonication process.

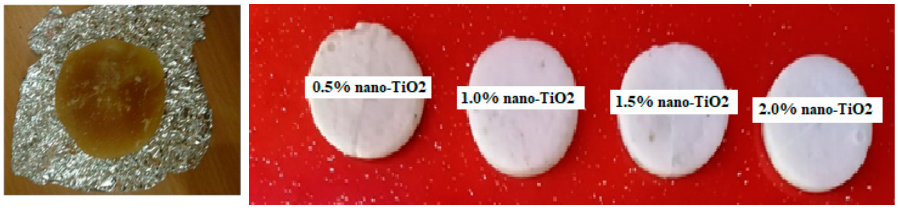

Figure 3. Samples of paraffin and nano-paraffins used in the study.

Nano-paraffin and nanofluids thermophysical properties. Tables 6 and 7 represent the measured thermophysical specifications of the prepared nanofluids and nano-paraffin. In the next section, these properties will be discussed in detail.

Table 6. The thermophysical specification of the tested nanofluids at 25 °C.

Nanofluid Mass Fraction (%)	TC (W/m K)	Density (g/cm^3)	Viscosity (mPa·s)	Stability Zeta Potential (mV)
Water	0.6	1.00	1.00	-
Nano-TiO_2 (%) 0.5	0.82	1.0125	1.013	68
Nano-TiO_2 (%) 1.0	1.13	1.019	1.023	64
Nano-TiO_2 (%) 1.5	1.25	1.022	1.028	59
Nano-TiO_2 (%) 2.0	1.36	1.025	1.033	48

Table 7. The thermophysical properties of tested nano-paraffin at 65 °C.

Nanofluid Type Mass Fraction (%)	TC (W/m K)	Density (g/cm^3)	Viscosity (mPa·s)	Stability TC Degradation (days)
Paraffin	0.2	950	0.088–0.077	-
Nano-TiO_2 (%) 0.5	0.31	961.4	0.09–0.082	98
Nano-TiO_2 (%) 1.0	0.48	967.86	0.92–0.085	94
Nano-TiO_2 (%) 1.5	0.54	970.14	0.094–0.088	89
Nano-TiO_2 (%) 2.0	0.66	972.61	0.0955–0.09	88

3.1. Thermal Conductivity

TC increased when the mass fraction of added nano-TiO_2 was increased, in both water and paraffin. Titanium oxide is a highly conductive metal oxide, so adding its nanoparticles to water caused a clear enhancement of the nanofluid TC, amounting to 36.6%, 88.3%, 108.3%, and 126.6%, resulting from 0.5%, 1.0%, 1.5%, and 2% nano-TiO_2 mass fractions added to water, respectively. As for paraffin, a quite remarkable increase in its TC at room temperature (25 °C) was measured. Of course, conductivity of the liquid state decreases by a certain percentage, but with nano-additives it remains high. Reference [59] found a decrease in the maximum value of TC when the material reached the phase change stat; after completing this change, the conductivity increased in both paraffin alone and with nano additives. Nano-TiO_2 addition caused increments in the TC of nano-paraffin by 55%, 140%, 170%, and 230%, from 0.5%, 1.0%, 1.5%, and 2% nano-TiO_2 mass fractions added to paraffin, respectively. These results indicate that the addition of nano-TiO_2 to paraffin is more efficient than adding it to water, because of paraffin's solid state at the measured temperature.

3.2. Density

The nanofluid and nano-paraffin density increased with the addition of nanoparticles. However, as the added nanoparticles mass fractions were small, the resulted density variations were also small. For the nanofluids, the density increments were 1.25%, 1.9%, 2.2%, and 2.5%, from 0.5%, 1.0%, 1.5%, and 2% nano-TiO_2 mass fractions added to water, respectively. Likewise, for paraffin, the addition of 0.5%, 1.0%, 1.5%, and 2% nano-TiO_2 mass fractions caused its density to increase by 1.2%, 1.88%, 2.12%, and 2.38%, respectively.

3.3. Viscosity

Viscosity expresses the resistance of a fluid to flow when there is a pressure difference that forces it to move. In PV/T applications, when paraffin is used, there is no movement, so the effect of viscosity here is very limited. However, the state of paraffin changes from solid to liquid during the melting process (charging), and then from liquid to solid during the solidification process (discharge). Viscosity plays an important role during the liquid paraffin period, as nanoparticle dispersion depends on it. Therefore, this property was studied during the increase in temperature of the nano-paraffin, to ensure its behavior during this period. Table 7 shows the results of the change in viscosity of the heat storage materials (paraffin and nano-paraffin) when temperatures were raised from 25 °C to 65 °C. These temperatures were chosen because they are the temperatures at which PV/T systems operate in most locations. The results showed that the viscosities of nano-paraffin with variable mass fractions are close, because the mass fractions of nanoparticles added are very small. The addition of NanoTiO_2 increased viscosity, whether liquid or solid, compared to paraffin. The viscosity of nano-paraffin decreased rapidly when the temperature increased (due to its TC amelioration compared to paraffin, as well as the improvement of thermal energy diffusion during heating). The decrease in density and viscosity with increasing temperatures (Table 7) means that water and nanofluid circulation pumps do not need to draw additional electrical power. This result is a positive one for any large system, as its generated power will not be affected because of circulating nanofluid with higher viscosity and density; these two characteristics will decrease with higher operating temperatures during the day.

3.4. Nanofluid Stability

In this study, a zeta potential analysis was adopted to measure the stability of the prepared suspensions, while another method was adopted to measure the stability of nano-paraffin, as will be explained in the next paragraph. In this technique, the change of electric charges in the nanofluid is measured, as the oppositely charged nanoparticles are attracted to the free charges. This process takes place in the nanofluid. The zeta potential values express the stability of the measured nanofluid. For example, a zeta value of more

than 60 mV expresses very high stability of the nano-suspension. In the case of a zeta limit between 40 and 60 mV, the stability of the nanofluid performs well. However, if the zeta voltage drops to between 30 and 40 millivolts, the nano-suspension is considered to have acceptable stability. If the zeta potential reaches less than 30 mV, the nano-suspension is considered unstable. Table 6 shows the zeta potential measurement of the prepared nanofluids. All prepared suspensions had a small mass fraction, so their stability was high, and the most stable suspension was that with a mass fraction of (0.5%). The addition of nano-TiO_2 particles with minute sizes (20 to 50 nm) and a high surface area, carefully dispersed using the sonication technique, which lasted for a sufficient time, caused uniform and fair distribution in the base liquid. The lowest zeta potential (48 mV) was observed in the case of adding 2% nano-TiO_2 to water. This zeta potential indicates that the nanofluid has a very good stability.

3.5. Nano-Paraffin Stability

The stability of any nano-paraffin production presents a real challenge. Today, with the use of mixing by sonication, for sufficient duration, and the use of small-sized nanoparticles, this process has become easier, and nano-paraffin product have high stability. The processed nano-paraffin undergoes a large number of repeated heating and cooling processes for a long period of time. The instability of nano-paraffin causes the deterioration of its thermal conductivity with time, which negatively affects the performance of the PV/T system. The success of using nano-paraffin in PV/T systems depends entirely on enhancing the mixing of nano-particles with paraffin and the stability of the mixture for a long period of time, while reducing costs. In this study, the method used by reference [59], in which the thermal conductivity of nano-paraffin is measured at equal time intervals, was adopted to determine to what extent it can be effectively used. There is a high potential for the agglomeration and deposition of nanoparticles in a nano-paraffin tank, and the most appropriate course of treatment is the optimum distribution of the particles through all the paraffin in the tank. Due to limited study time, conductivity deterioration by 5% was adopted as an indicator of declining stability, with the possibility of utilizing this mixture (Nano-paraffin) until its conductivity decreased to 30%, after which it would be safer to re-mix again, so as not to affect the performance of the PV/T system.

The results listed in Table 7 show that the stability of nano-paraffin mixtures was very good, and exceeded 85 days before their conductivity decreased by 5%. This result indicates the possibility of using it for long periods before emptying the mixture from the tank and re-mixing it again. The highest stability was recorded for the 0.5% mass fraction-added mixture (98 days), and the lowest was recorded for the 2% mixture (88 days). From here, it is possible to confirm the success of the method used in this study for mixing nano-TiO_2 with paraffin, as well as the good selection of materials and mixing time.

3.6. PV/T System Performance

Figure 4 shows the change in solar radiation intensity during the time of the experiments. The figure illustrates the data measured on site. It can be noticed from the figure that the solar radiation intensity in the city of Baghdad is very high, and its peak is between 12 PM and 2 PM, when it reaches about 950 W/m^2. Solar radiation fluctuates as a result of environmental conditions, such as the movement of clouds and air masses, so the rise and fall of this intensity is not consistent. This high irradiance is preferred for the production of photovoltaic electricity (close to 1000 W/m^2 under standard conditions). However, the ambient temperature is higher than standard conditions (25 °C), reaching about 40 °C. These conditions cause the temperature of the photovoltaic panels to rise, which leads to deterioration of the power levels generated by them.

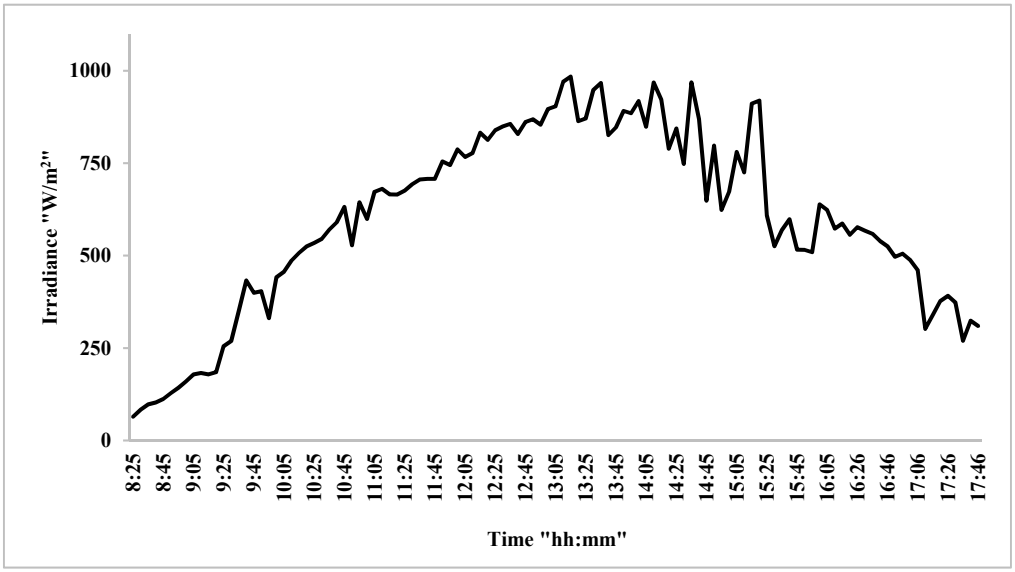

Figure 4. The variation of solar radiation intensity with time.

The first practical experiments were conducted to define the most suitable flow rate of coolant (whether water or nanofluid) in the heat exchanger. Therefore, this flow was changed to several settings by adjusting the locking hole and measuring the fluid mass flow rate (Figure 5). The flow rates of water and nanofluids were measured using HC (US Hunter), with an uncertainty of ±0.55 (as illustrated in Table 5). The experiments were performed using water. Figure 4 demonstrates that the rising fluid flow rate caused a reduction in PV module body temperature. The increase in mass flow rate caused an increase in absorbed heat; however, as the vibration begins to occur in the system along with a large increase in flowing mass, there are limits to this increase. The results show that the best photovoltaic panel temperature reduction occurred when 0.175 kg/s (Re No. = 308,000) was used, but the vibration accompanying this flow caused it to work better at the lower flow rate of 0.15 kg/s (Re No. = 282,000), without vibration of the system. All of the following experiments took place at this flow rate.

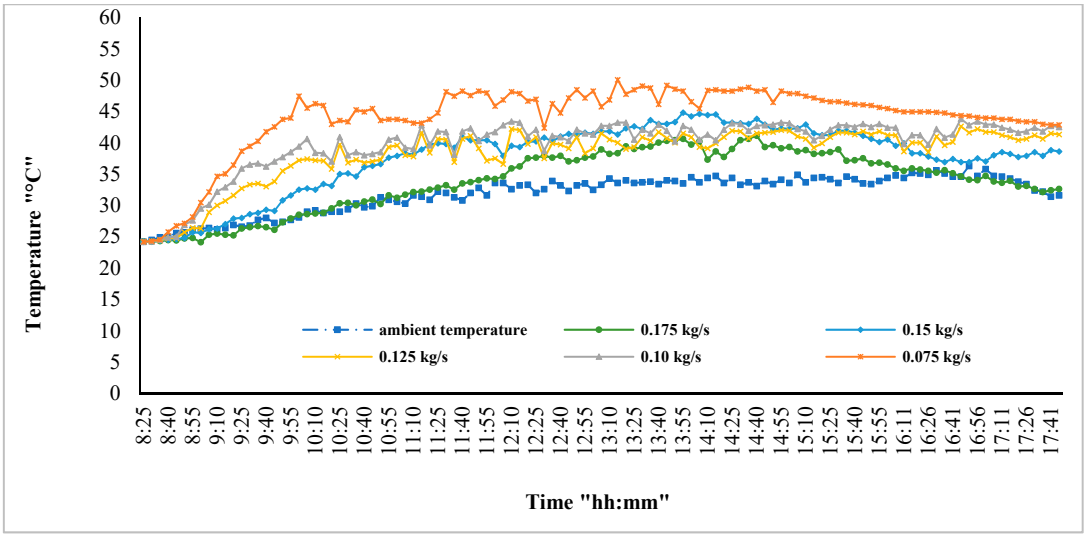

Figure 5. Water mass flow rate effect on PV module surface temperature.

Figure 6 shows the PV module surface temperature variations according to the change in the type of cooling used. The standalone PV module reached its highest possible

temperatures (above 55 °C) at peak time, from 12 PM to 3 PM. When cooling this module with water, its temperatures dropped significantly at peak time, reaching 45 °C (10 °C less, on average). When using the nano-fluid and nano-paraffin PV/T system, the temperature decreased further, reaching 36 °C (an average of 19 °C less than the standalone PV panel).

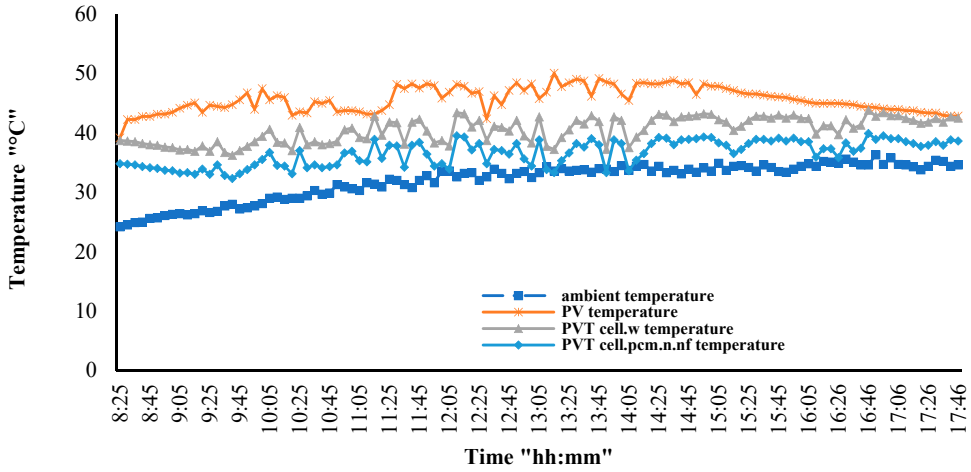

Figure 6. Cooling effect of the PV/T systems compared to the standalone PV module.

The proposed PV/T system (nano-paraffin and nano-fluid) has superior cooling capabilities than the water-cooled PV/T system alone. From the figure, it can be seen that, for the period before 9 AM, the nanofluid-nano-paraffin cooling is limited, and the module temperature is high. This phenomenon can be explained by the fact that the paraffin temperature, at this time, didn't reach the melting point, and the differences between the PV surface and paraffin temperatures were small. However, despite this, the temperature of the PV/T module remained lower than the temperature of the standalone PV.

Figure 7 shows the effect of the changing surface temperature of the PV module, due to weather conditions and exposure time, on the PV modules voltage. The shape of the voltage waves for both PV and PV/T systems is significantly increased by an increase in the intensity of the solar radiation, and this change is greater than the current condition, as mentioned by many studies [11,33,38]. The figure shows the presence of fluctuations in the voltage wave with time, as a result of the changing intensity of solar radiation, which is clearer in the case of the standalone PV module, while the PV/T system (nano-fluid and nano-paraffin) is flatter with the change of time. Any change, even a small one, in solar radiation intensity directly affects the generated electrical voltage. The measured voltages range from 10–11 V in the case of a standalone PV module, 12–13 V in the case of a water-cooled PV/T system, and 16–18 V in the case of nano-paraffin and nanofluid PV/T system.

Here it must be explicitly stated that the energy spent by the water and nanofluid circulating pumps was not included in the calculations of energy consumption of the photovoltaic modules studied. This behavior was due to the use of one panel as a representative of each studied system (the produced power of the panels is limited), which reduced the productivity of the panels and hindered fair comparison between them. In the case of larger systems, the consumption of the circulation pump must certainly be included in the calculations.

Figure 8 shows the differences in electrical efficiency among the studied systems. The standalone PV module efficiency is highest in the early morning, then decreases, reaching its lowest values at peak time, but recovers some of its losses before sunset. The dependence of this module on air cooling and its movement is not guaranteed, especially in the city of Baghdad, as wind speed ranges from 0 m/s to a maximum of 3 m/s, which caused significant heating of this module and a clear reduction in electrical efficiency. As for the PV/T system (water-cooled), its electrical efficiency is higher than the previous case,

with an average of 30.9% for a full-day operation. The curves show that the electrical efficiency of this system declined at peak time. As for the last case (the nano-fluid and nano-paraffin cooled PV/T system), the electrical efficiency is higher by an average of 106.5% and 57.7% compared to the two previous cases (the standalone PV and water-cooled PV/T systems), respectively. This result demonstrates the high efficiency of the cooling process in this system.

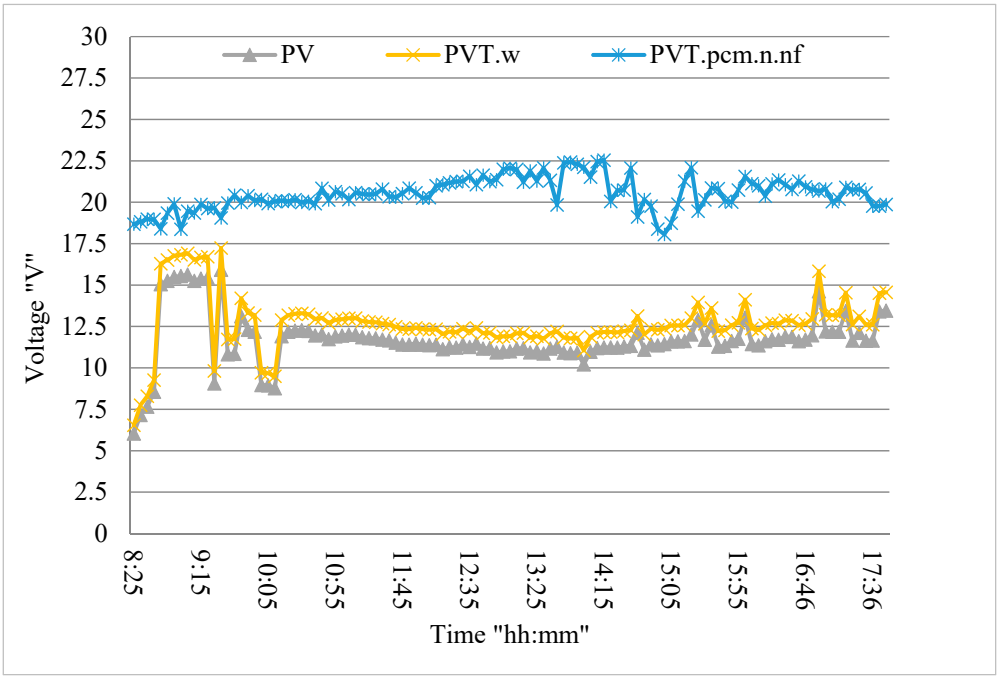

Figure 7. The tested systems' voltage variation with time.

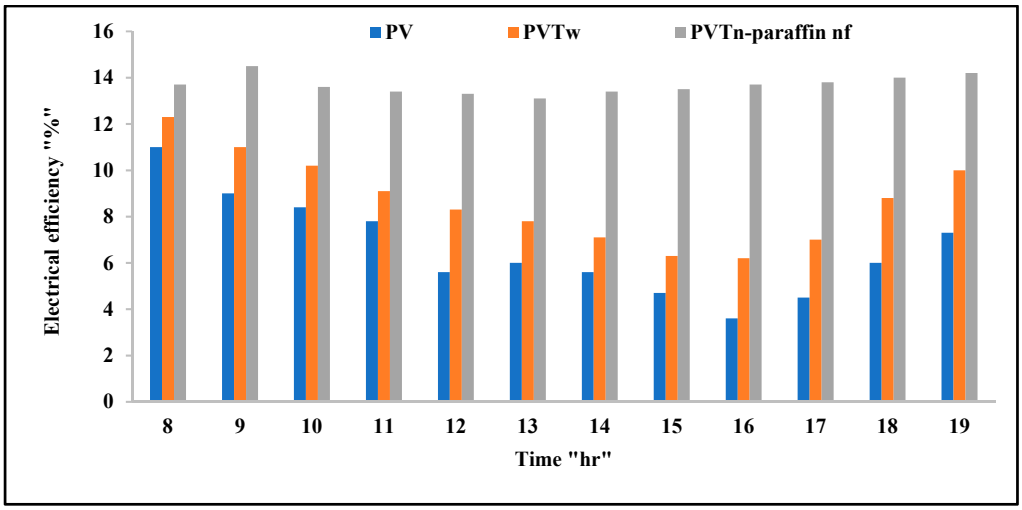

Figure 8. The electrical efficiencies of the tested systems variations with time.

Figure 9 shows the differences in thermal efficiency among the studied systems. There is no thermal efficiency for the standalone PV module, as the heat absorbed from it is not utilized. As for the case of PV/T systems, this heat can be collected and used in many applications, the most important of which being heating water for domestic purposes, to heat swimming pools, or in solar stills. The water-cooled PV/T system efficiency is lowest in the early morning, reaches its maximum values at peak time, and decreases, relatively, after that until sunset. In the case of the nanofluid and nano-paraffin PV/T system, the thermal efficiency is little, and almost equal to the previous system, in the early morning hours, but it increases clearly and exceeds the previous system by 43.7% during peak period. This result supports our previously reached conclusion, which is that the cooling process of this system is very efficient.

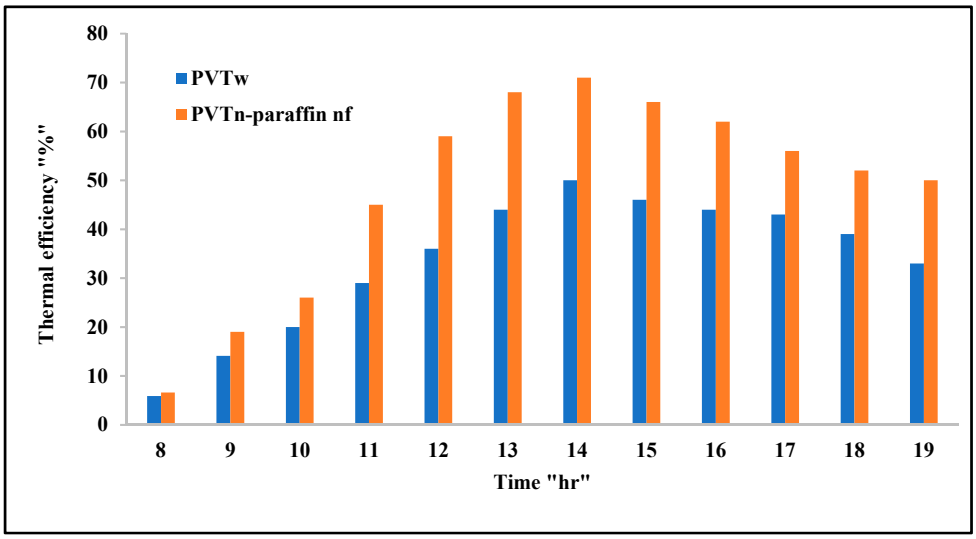

Figure 9. Variations of the thermal efficiencies of the tested systems with time.

Figure 10 shows that the nano-paraffin nanofluid PV/T system produced the highest total efficiency compared to the other two studied systems. This system, which had the highest cooling capacity for the photovoltaic panel, compared to the other systems (Figure 5), produced the highest thermal efficiency (Figure 8) and electrical efficiency (Figure 7), and, as a result, its total efficiency was the greatest. The total efficiency is the sum of the electrical and thermal efficiencies, so we find that it is the highest possible during the peak period (from 12–4 PM) for the two studied PV/T systems, while for the case of the PV system it is at its lowest values, because this system does not cool and does not have thermal efficiency. The highest total efficiency was 84.4%, for the nano-paraffin and nanofluid PV/T system, at 2 PM. When cooling with water, the maximum total efficiency was 57.1%, at the same hour. As for the highest total efficiency of the standalone PV system, it was 11% at eight o'clock in the morning, and this efficiency indicates an electrical efficiency. It is the highest possible at the coolest temperature of the PV panel, which is of course the beginning of exposure to solar radiation.

3.7. Comparison with Other Works from Literature

Figure 11 shows the ameliorations in the TC of different types of nanofluids for variables studies from the literature. The results show that nanofluids prepared from water + nano-TiO_2 (recent study) provide the best TC enhancement rate. The reason for this (despite the presence of nanoparticles with a higher conductivity than nano-TiO_2) is the use of particles of small size, which can stay suspended for as long as possible. In addition, the sonication process used was successful in terms of shaking speed and duration.

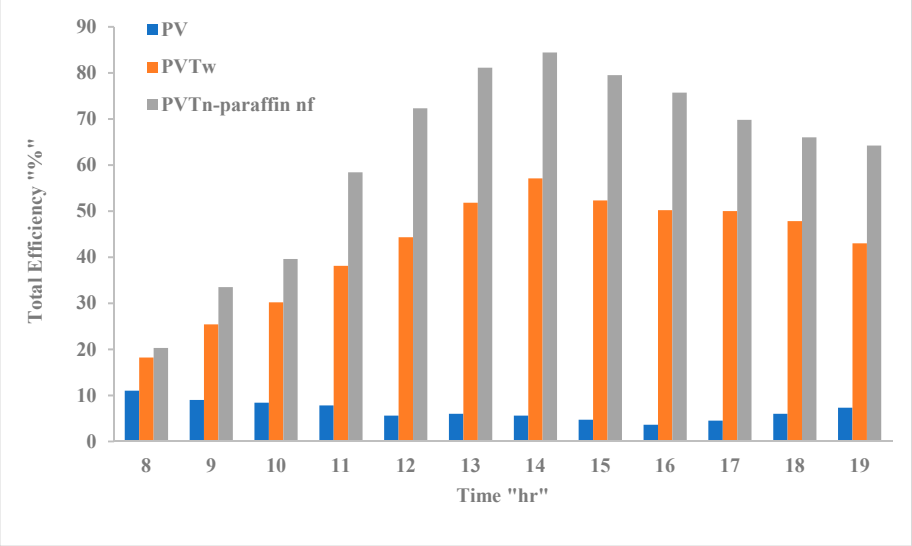

Figure 10. The total efficiencies of the tested systems variations with time.

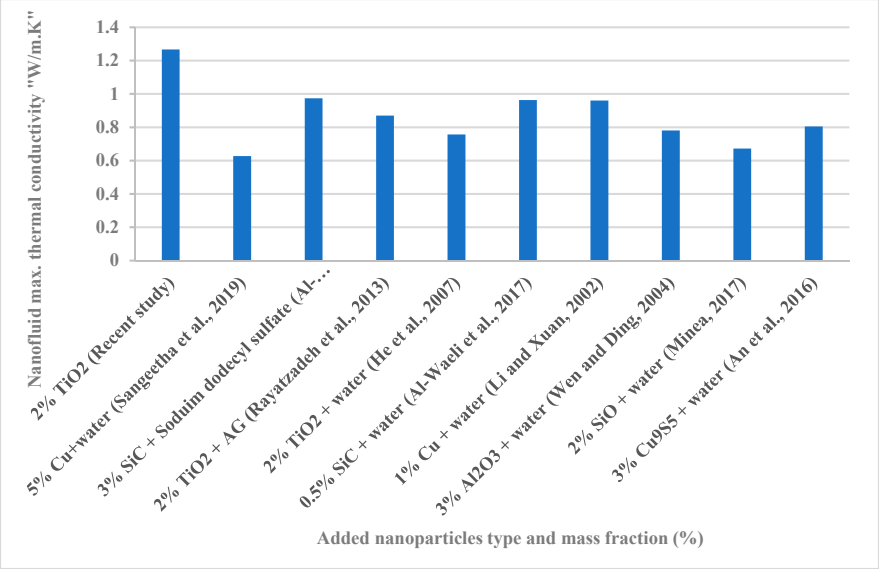

Figure 11. Comparison between the present study and other works in the literature, regarding nanofluid TC enhancement Sangeetha et al., 2019 [10]; Al-Waeli et al, 2019 [20]; Rayatzadeh et al., 2013 [32]; He et al., 2007 [49]; Al-Waeli et al., 2017 [57]; Li and Xuan, 2002 [60]; Wen and Ding, 2004 [61]; Minea, 2017 [62] and An et al., 2016 [63].

Figure 12 shows the improvement in the TC of several different types of nano-PCMs. The results show that the nano-paraffin prepared in this study provided a clear improvement in TC, and ranked second after the results of reference [64]. The successful mixing process and quality of the PCM used, in addition to the quality of the nanoparticles, are the reasons for obtaining a stable nano-PCM with a high TC. The results show the probability of enhancement using paraffin, among all types of PCMs used.

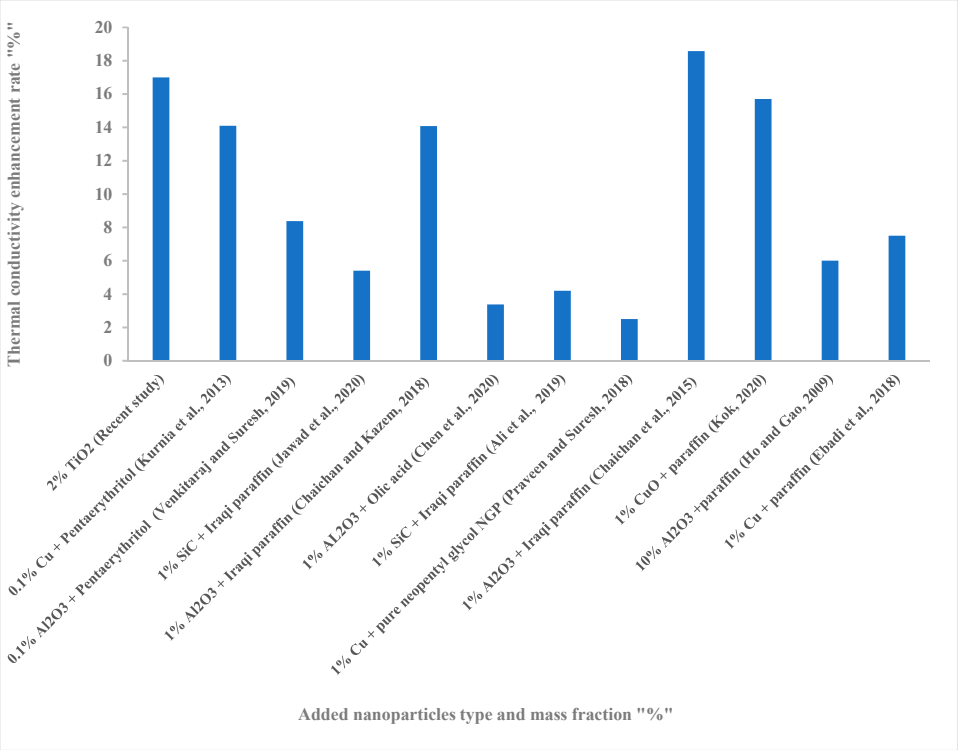

Figure 12. Comparison between the present study and other works in the literature, regarding nano-PCM TC enhancement Kurnia et al., 2013 [65]; Venkitaraj and Suresh, 2019 [66]; Jawad et al., 2020 [67]; Chaichan and Kazem, 2018 [68]; Chen et al., 2020 [44]; Ali et al., 2019 [69]; Praveen and Suresh, 2018 [70]; Chaichan et al., 2015 [64]; Kok, 2020 [71], Ho and Gao, 2009 [72] and Ebadi et al., 2018 [73].

4. Conclusions

Most of the time, the weather in Iraq is dusty, hot, and highly radioactive. These matters limit the possibility of relying on PV power plants with high capacities. In this study, a practical attempt is made to reduce the PV module's temperatures by cooling them in two different methods, the first using a cooling fluid (water), while in the second a system consisting of a thermal tank containing nano-paraffin and cooled with a nanofluid was employed. Nano-TiO_2 was selected, for its particles of small size and diameter, to be added to water and paraffin. This addition significantly improved the TC of water (126% higher compared to water, when 2% Nano-TiO_2 was added). In addition, the paraffin TC was improved by up to 170% at the same mass fraction of added nanoparticles. The results of the study show a clear decrease in the temperature of the photovoltaic panel of the proposed system compared to the water-cooled PV/T system or standalone PV system. During peak time (from 12 PM to 3 PM), the temperature of the PV panel decreased by about 19 °C. The proposed system produced the highest electrical efficiency, with an increase of 106% and 56% compared to the standalone PV panel and water-cooled system, respectively. The nano-system achieved 43% higher thermal efficiency than the water-cooled system.

Author Contributions: Conceptualization, M.T.C. and A.A.A.; methodology, M.T.C.; validation, H.A.K., W.N.R.W.I. and M.S.T.; formal analysis, H.A.K. and W.N.R.W.I.; investigation, M.S.T.; resources, H.A.K., W.N.R.W.I. and M.S.T.; data curation, H.A.K., W.N.R.W.I. and M.S.T.; writing—original draft preparation, M.T.C. and A.A.A.; writing—review and editing, A.A.H.K., M.T.C. and A.A.A.; supervision, M.T.C. and A.A.A.; project administration, M.T.C., A.A.H.K. and A.A.A.; funding acquisition, H.A.K., W.N.R.W.I. and M.S.T. All authors have read and agreed to the published version of the manuscript.

Funding: This research received no external funding.

Data Availability Statement: Not applicable.

Acknowledgments: We acknowledge UKM for support.

Conflicts of Interest: The authors declare no conflict of interest.

References

1. Ahmed, W.K.; Abed, T.A.; Salam, A.Q.; Reza, K.S.; Mahdiy, M.T.; Chaichan, M.T. Environmental Impact of Using Generators in the University of Technology in Baghdad, Iraq. *J. Therm. Eng.* **2020**, *6*, 272–281. [CrossRef]
2. Chaichan, M.T.; Kazem, H.A.; Abed, T. Traffic and outdoor air pollution levels near highways in Baghdad, Iraq. *Environ. Dev. Sustain.* **2018**, *20*, 589–603. [CrossRef]
3. Chaichan, M.T.; Kazem, H.A. *Generating Electricity Using Photovoltaic Solar Plants in Iraq*; Springer International Publishing: Cham, Switzerland, 2018; pp. 47–82.
4. Kazem, H.A.; Chaichan, M.T.; Al-Waeli, A.H.; Sopian, K. A review of dust accumulation and cleaning methods for solar photovoltaic systems. *J. Clean. Prod.* **2020**, *276*, 123187. [CrossRef]
5. Alnasser, T.M.; Mahdy, A.M.; Abass, K.I.; Chaichan, M.T.; Kazem, H.A. Impact of dust ingredient on photovoltaic performance: An experimental study. *Sol. Energy* **2020**, *195*, 651–659. [CrossRef]
6. Chaichan, M.T.; Kazem, H.A. Experimental evaluation of dust composition impact on photovoltaic performance in Iraq. *Energy Sources, Part A Recover. Util. Environ. Eff.* **2020**, 1–22. [CrossRef]
7. Al-Waeli, A.H.; Sopian, K.; Kazem, H.A.; Chaichan, M.T. Photovoltaic solar thermal (PV/T) collectors past, present and future: A review. *Int. J. Appl. Eng. Res.* **2016**, *11*, 10757–10765.
8. Al-Damook, M.; Al Qubeissi, M.; Khatir, Z.; Dixon-Hardy, D.; Heggs, P.J. Thermal and Electrical Performance Evaluation and Design Optimization of Hybrid PV/T Systems. In *Advances in Heat Transfer and Thermal Engineering*; Springer Science and Business Media LLC: Berlin/Heidelberg, Germany, 2021; pp. 805–813.
9. Gao, Z.; Yu, N.; Cao, X.; Sun, L.; Zhou, J.; Yuan, Y. *A Comparison Study on Energy Performance between Different PV/T Systems and PV System in Highland Cold Winter. T Systems and PV System in Highland Cold Winter*; SSRN: Rochester, NY, USA, 2021.
10. Sangeetha, M.; Manigandan, S.; Chaichan, M.T.; Kumar, V. Progress of MWCNT, Al_2O_3, and CuO with water in enhancing the photovoltaic thermal system. *Int. J. Energy Res.* **2019**, *44*, 821–832. [CrossRef]
11. Xu, H.; Wang, N.; Zhang, C.; Qu, Z.; Karimi, F. Energy conversion performance of a PV/T-PCM system under different thermal regulation strategies. *Energy Convers. Manag.* **2021**, *229*, 113660. [CrossRef]
12. Chaichan, M.T.; Abaas, K.I.; Kazem, H.A. Design and assessment of solar concentrator distillating system using phase change materials (PCM) suitable for desertic weathers. *Desalination Water Treat.* **2015**, *57*, 1–11. [CrossRef]
13. Charalambous, P.G.; Maidment, G.G.; Kalogirou, S.A.; Yiakoumetti, K. Photovoltaic thermal (PV/T) collectors: A review. *Appl. Therm. Eng.* **2007**, *27*, 275–286. [CrossRef]
14. Kiran, S.; Devadiga, U. Performance Analysis of Hybrid PV/Thermal Systems. *Int. J. Emerg. Technol. Adv. Eng.* **2014**, *4*, 80–86.
15. Khanjari, Y.; Pourfayaz, F.; Kasaeian, A. Numerical investigation on using of nanofluid in a water-cooled photovoltaic thermal system. *Energy Convers. Manag.* **2016**, *122*, 263–278. [CrossRef]
16. Zhang, C.; Shen, C.; Wei, S.; Zhang, Y.; Sun, C. Flexible management of heat/electricity of novel PV/T systems with spectrum regulation by Ag nanofluids. *Energy* **2021**, *221*, 119903. [CrossRef]
17. Nkurikiyimfura, I.; Wang, Y.; Safari, B.; Nshingabigwi, E. Electrical and thermal performances of photovoltaic/thermal systems with magnetic nanofluids: A review. *Particuology* **2021**, *54*, 181–200. [CrossRef]
18. Al-Waeli, A.H.A.; Kazem, H.A.; Sopian, K.; Chaichan, M.T. Techno-economical assessment of grid connected PV/T using nanoparticles and water as base-fluid systems in Malaysia. *Int. J. Sustain. Energy* **2018**, *37*, 558–575.
19. Gupta, S.K.; Pradhan, S. A review of recent advances and the role of nanofluid in solar photovoltaic thermal (PV/T) system. *Mater. Today Proc.* **2021**, *44*, 782–791.
20. Alwaeli, A.H.A.; Chaichan, M.T.; Sopian, K.; Kazem, H.A. Influence of the base fluid on the thermo-physical properties of PV/T nanofluids with surfactant. *Case Stud. Therm. Eng.* **2019**, *13*, 100340.
21. Purohit, N.; Jakhar, S.; Gullo, P.; Dasgupta, M.S. Heat transfer and entropy generation analysis of alumina/water nanofluid in a flat plate PV/T collector under equal pumping power comparison criterion. *Renew. Energy* **2018**, *120*, 14–22. [CrossRef]
22. Chaichan, M.T.; Kazem, H.A.; Al-Waeli, A.H.; Sopian, K. Controlling the melting and solidification points temperature of PCMs on the performance and economic return of the water-cooled photovoltaic thermal system. *Sol. Energy* **2021**, *224*, 1344–1357. [CrossRef]
23. Vakhshouri, A.R. *Paraffin as Phase Change Material*; IntechOpen: London, UK, 2018; pp. 1–23.
24. Chaichan, M.T.; Kazem, H.A. Using Aluminum Powder with PCM (paraffin wax) to Enhance Single Slope Solar Water Distillation Productivity in Baghdad-Iraq Winter Weathers. *Int. J. Renew. Energy Res.* **2015**, *5*, 251–257.
25. Mahmoud, B.K.; Ibrahim, S.I.; Abass, K.I.; Ali, A.J.; Chaichan, M.T. Flat solar air heater collector with phase change materials for domestic purposes in Iraqi climate. *IOP Conf. Ser. Mater. Sci. Eng.* **2020**, *928*, 022099. [CrossRef]
26. Habib, N.A.; Ali, A.J.; Chaichan, M.T.; Kareem, M. Carbon nanotubes/paraffin wax nanocomposite for improving the performance of a solar air heating system. *Therm. Sci. Eng. Prog.* **2021**, *23*, 100877. [CrossRef]

27. Shojaeefard, M.H.; Sakran, N.B.; Sharfabadi, M.M.; Davoudi, N. A Novel Review on Nano-fluid and Phase Change Material based Photovoltaic Thermal (PV/T) Systems. *IOP Conf. Series: Mater. Sci. Eng.* **2021**, *1067*, 012099. [CrossRef]
28. Khodadadi, M.; Sheikholeslami, M. Numerical simulation on the efficiency of PVT system integrated with PCM under the influence of using fins. *Sol. Energy Mater. Sol. Cells* **2021**, *233*, 111402. [CrossRef]
29. Rossi, R.M.; Bolli, W.P. Phase Change Materials for the Improvement of Heat Protection. *Adv. Eng. Mater.* **2005**, *7*, 368–373. [CrossRef]
30. Fallahi, A.; Guldentops, G.; Tao, M.; Granados-Focil, S.; Van Dessel, S. Review on solid-solid phase change materials for thermal energy storage: Molecular structure and thermal properties. *Appl. Therm. Eng.* **2017**, *127*, 1427–1441. [CrossRef]
31. Nazir, H.; Batool, M.; Osorio, F.J.B.; Isaza-Ruiz, M.; Xu, X.; Vignarooban, K.; Phelan, P.; Kannan, A.M. Recent developments in phase change materials for energy storage applications: A review. *Int. J. Heat Mass Transf.* **2019**, *129*, 491–523. [CrossRef]
32. Rayatzadeh, H.R.; Saffar-Avval, M.; Mansourkiaei, M.; Abbassi, A. Effects of continuous sonication on laminar convective heat transfer inside a tube using water–TiO_2 nanofluid. *Exp. Therm. Fluid Sci.* **2013**, *48*, 8–14. [CrossRef]
33. Al-Waeli, A.H.; Kazem, H.A.; Chaichan, M.T.; Sopian, K. *Photovoltaic/Thermal (PV/T) Systems: Principles, Design, and Applications*; Springer Nature: Cham, Switzerland, 2019.
34. Ho, C.J.; Gao, J. An experimental study on melting heat transfer of paraffin dispersed with Al_2O_3 nanoparticles in a vertical enclosure. *Int. J. Heat Mass Transf.* **2013**, *62*, 2–8. [CrossRef]
35. Mishra, A.K.; Lahiri, B.; Philip, J. Thermal conductivity enhancement in organic phase change material (phenol-water system) upon addition of Al_2O_3, SiO_2 and TiO_2 nano-inclusions. *J. Mol. Liq.* **2018**, *269*, 47–63. [CrossRef]
36. Colangelo, G.; Favale, E.; Miglietta, P.; Milanese, M.; de Risi, A. Thermal conductivity, viscosity and stability of Al_2O_3 -diathermic oil nanofluids for solar energy systems. *Energy* **2016**, *95*, 124–136. [CrossRef]
37. Hamid, K.A.; Azmi, W.; Nabil, M.; Mamat, R. Experimental investigation of nanoparticle mixture ratios on TiO_2–SiO_2 nanofluids heat transfer performance under turbulent flow. *Int. J. Heat Mass Transf.* **2018**, *118*, 617–627. [CrossRef]
38. Azmi, W.; Hamid, K.A.; Usri, N.; Mamat, R.; Sharma, K. Heat transfer augmentation of ethylene glycol: Water nanofluids and applications—A review. *Int. Commun. Heat Mass Transf.* **2016**, *75*, 13–23. [CrossRef]
39. Sharar, D.J.; Donovan, B.F.; Warzoha, R.J.; Wilson, A.A.; Leff, A.C.; Hanrahan, B.M. Solid-state thermal energy storage using reversible martensitic transformations. *Appl. Phys. Lett.* **2019**, *114*, 143902. [CrossRef]
40. Iacobazzi, F.; Milanese, M.; Colangelo, G.; De Risi, A. A critical analysis of clustering phenomenon in Al_2O_3 nanofluids. *J. Therm. Anal.* **2019**, *135*, 371–377. [CrossRef]
41. Zawawi, N.N.M.; Azmi, W.; Redhwan, A.; Sharif, M.; Sharma, K.V. Thermo-physical properties of Al_2O_3-SiO_2/PAG composite nanolubricant for refrigeration system. *Int. J. Refrig.* **2017**, *80*, 1–10. [CrossRef]
42. Ghadimi, A.; Saidur, R.; Metselaar, H.S.C. A review of nanofluid stability properties and characterization in stationary conditions. *Int. J. Heat Mass Transf.* **2011**, *54*, 4051–4068. [CrossRef]
43. Afzal, A.; Nawfal, I.; Mahbubul, I.M.; Kumbar, S.S. An overview on the effect of ultrasonication duration on different properties of nanofluids. *J. Therm. Anal.* **2018**, *135*, 393–418. [CrossRef]
44. Chen, Z.; Shahsavar, A.; Al-Rashed, A.A.; Afrand, M. The impact of sonication and stirring durations on the thermal conductivity of alumina-liquid paraffin nanofluid: An experimental assessment. *Powder Technol.* **2020**, *360*, 1134–1142. [CrossRef]
45. Alwaeli, A.H.A.; Chaichan, M.T.; Kazem, H.A.; Sopian, K.; Safaei, J. Numerical study on the effect of operating nanofluids of photovoltaic thermal system (PV/T) on the convective heat transfer. *Case Stud. Therm. Eng.* **2018**, *12*, 405–413. [CrossRef]
46. Babu, J.R.; Kumar, K.K.; Rao, S.S. State-of-art review on hybrid nanofluids. *Renew. Sustain. Energy Rev.* **2017**, *77*, 551–565. [CrossRef]
47. Li, D.; Fang, W.; Feng, Y.; Geng, Q.; Song, M. Stability properties of water-based gold and silver nanofluids stabilized by cationic gemini surfactants. *J. Taiwan Inst. Chem. Eng.* **2019**, *97*, 458–465. [CrossRef]
48. Moldoveanu, G.M.; Huminic, G.; Minea, A.A.; Huminic, A. Experimental study on thermal conductivity of stabilized Al_2O_3 and SiO_2 nanofluids and their hybrid. *Int. J. Heat Mass Transf.* **2018**, *127*, 450–457. [CrossRef]
49. He, Y.; Jin, Y.; Chen, H.; Ding, Y.; Cang, D.; Lu, H. Heat transfer and flow behaviour of aqueous suspensions of TiO_2 nanoparticles (nanofluids) flowing upward through a vertical pipe. *Int. J. Heat Mass Transf.* **2007**, *50*, 2272–2281. [CrossRef]
50. Khairul, M.; Shah, K.; Doroodchi, E.; Azizian, R.; Moghtaderi, B. Effects of surfactant on stability and thermo-physical properties of metal oxide nanofluids. *Int. J. Heat Mass Transf.* **2016**, *98*, 778–787. [CrossRef]
51. Al-Waeli, A.H.; Chaichan, M.T.; Kazem, H.A.; Sopian, K.; Ibrahim, A.; Mat, S.; Ruslan, M.H. Comparison study of indoor/outdoor experiments of a photovoltaic thermal PV/T system containing SiC nanofluid as a coolant. *Energy* **2018**, *151*, 33–44. [CrossRef]
52. Lewis, R.J., Sr. *Hazardous Chemical Desk Reference*; Wiley: Hoboken, NJ, USA, 2008.
53. Lai, Y.-K.; Sun, L.; Chen, Y.; Zhuang, H.; Lin, C.; Chin, J.W. Effects of the Structure of TiO_2 Nanotube Array on Ti Substrate on Its Photocatalytic Activity. *J. Electrochem. Soc.* **2006**, *153*, D123–D127. [CrossRef]
54. Goia, F.; Zinzi, M.; Carnielo, E.; Serra, V. Characterization of the optical properties of a PCM glazing system. *Energy Procedia* **2012**, *30*, 428–437. [CrossRef]
55. Atal, A.; Wang, Y.; Harsha, M.; Sengupta, S. Effect of porosity of conducting matrix on a phase change energy storage device. *Int. J. Heat Mass Transf.* **2016**, *93*, 9–16. [CrossRef]
56. Alwaeli, A.H.A.; Chaichan, M.T.; Sopian, K.; Kazem, H.A.; Mahood, H.B.; Khadom, A.A. Modeling and experimental validation of a PVT system using nanofluid coolant and nano-PCM. *Sol. Energy* **2019**, *177*, 178–191. [CrossRef]

57. Al-Waeli, A.H.; Chaichan, M.T.; Kazem, H.A.; Sopian, K. Evaluation and analysis of nanofluid and surfactant impact on photovoltaic-thermal systems. *Case Stud. Therm. Eng.* **2019**, *13*, 100392. [CrossRef]
58. Holman, J.P. *Experimental Methods for Engineers*, 8th ed.; McGraw-Hill: New York, NY, USA, 2011.
59. Alwaeli, A.H.A.; Sopian, K.; Chaichan, M.T.; Kazem, H.A.; Ibrahim, A.; Mat, S.; Ruslan, M.H. Evaluation of the nanofluid and nano-PCM based photovoltaic thermal (PVT) system: An experimental study. *Energy Convers. Manag.* **2017**, *151*, 693–708. [CrossRef]
60. Li, Q.; Xuan, Y. Convective heat transfer and flow characteristics of Cu–water nanofluid. *Sci. China Ser. E Technol. Sci.* **2002**, *45*, 408–416.
61. Wen, D.; Ding, Y. Experimental investigation into convective heat transfer of nanofluids at the entrance region under laminar flow conditions. *Int. J. Heat Mass Transf.* **2004**, *47*, 5181–5188. [CrossRef]
62. Minea, A.A. Hybrid nanofluids based on Al_2O_3, TiO_2 and SiO_2: Numerical evaluation of different approaches. *Int. J. Heat Mass Transf.* **2017**, *104*, 852–860. [CrossRef]
63. An, W.; Wu, J.; Zhu, T.; Zhu, Q. Experimental investigation of a concentrating PV/T collector with Cu9S5 nanofluid spectral splitting filter. *Appl. Energy* **2016**, *184*, 197–206. [CrossRef]
64. Chaichan, M.T.; Kamel, S.H.; Al-Ajeely, A.N.M. Thermal conductivity enhancement by using nano-material in phase change material for latent heat thermal energy storage Systems. *Saussurea* **2015**, *5*, 48–55.
65. Kurnia, J.C.; Sasmito, A.P.; Jangam, S.V.; Mujumdar, A.S. Improved design for heat transfer performance of a novel phase change material (PCM) thermal energy storage (TES). *Appl. Therm. Eng.* **2013**, *50*, 896–907. [CrossRef]
66. Venkitaraj, K.P.; Suresh, S. Effects of Al_2O_3, CuO and TiO_2 nanoparticles son thermal, phase transition and crystallization properties of solid-solid phase change material. *Mech. Mater.* **2019**, *128*, 64–88. [CrossRef]
67. Jawad, Q.A.; Mahdy, A.M.; Khuder, A.H.; Chaichan, M.T. Improve the performance of a solar air heater by adding aluminum chip, paraffin wax, and nano-SiC. *Case Stud. Therm. Eng.* **2020**, *19*, 100622. [CrossRef]
68. Chaichan, M.T.; Kazem, H.A. Single slope solar distillator productivity improvement using phase change material and Al_2O_3 nanoparticle. *Sol. Energy* **2018**, *164*, 370–381. [CrossRef]
69. Ali, A.H.; Ibrahim, S.I.; Jawad, Q.A.; Jawad, R.S.; Chaichan, M.T. Effect of nanomaterial addition on the thermophysical properties of Iraqi paraffin wax. *Case Stud. Therm. Eng.* **2019**, *15*, 100537. [CrossRef]
70. Praveen, B.; Suresh, S. Experimental study on heat transfer performance of neopentyl glycol/CuO composite solid-solid PCM in TES based heat sink. *Eng. Sci. Technol. Int. J.* **2018**, *21*, 1086–1094. [CrossRef]
71. Kok, B. Examining effects of special heat transfer fins designed for the melting process of PCM and Nano-PCM. *Appl. Therm. Eng.* **2020**, *170*, 114989. [CrossRef]
72. Ho, C.J.; Gao, J. Preparation and thermophysical properties of nanoparticle-in-paraffin emulsion as phase change material. *Int. Commun. Heat Mass Transf.* **2009**, *36*, 467–470. [CrossRef]
73. Ebadi, S.; Tasnim, S.H.; Aliabadi, A.A.; Mahmud, S. Geometry and nanoparticle loading effects on the bio-based nano-PCM filled cylindrical thermal energy storage system. *Appl. Therm. Eng.* **2018**, *141*, 724–740. [CrossRef]